Exploring the off-flavour removal mechanism of d-limonene, geraniol and acetophenone in perilla leaves from the perspective of molecular structure and kinetic properties

Ke Bi, Yue Liu, Kangyu Wang, Ping Yang, Dong Han, Chunhui Zhang, Yanlu Luan, Lijuan Dong, Prince Chisoro, Marie-laure Fauconnier

PII: S0308-8146(25)01189-6

DOI: https://doi.org/10.1016/j.foodchem.2025.143938

Reference: FOCH 143938

To appear in: *Food Chemistry*

Received date: 19 December 2024

Revised date: 22 February 2025

Accepted date: 16 March 2025

Please cite this article as: K. Bi, Y. Liu, K. Wang, et al., Exploring the off-flavour removal mechanism of d-limonene, geraniol and acetophenone in perilla leaves from the perspective of molecular structure and kinetic properties, *Food Chemistry* (2024), https://doi.org/10.1016/j.foodchem.2025.143938

Exploring the off-flavour removal mechanism of D-limonene, geraniol and acetophenone in perilla leaves from the perspective of molecular structure and kinetic properties

Ke Bi[a,b,1], Yue Liu[a,1], Kangyu Wang[a], Ping Yang[a], Dong Han[a,※], Chunhui Zhang[a,※], Yanlu Luan[c], Lijuan Dong[c], Prince Chisoro[a], Marie-laure Fauconnier[b]

[a]Key Laboratory of Agro-Products Processing, Ministry of Agriculture and Rural Affairs, Institute of Food Science and Technology, Chinese Academy of Agricultural Sciences, Beijing, 100193, China.

[b]Laboratory of Chemistry of Natural Molecules, Gembloux Agro-Bio Tech, University of Liege, 5030 Gembloux, Belgium.

[c]Yantai Fumeite Information Technology Co., Ltd.

[1] These authors contributed equally to this work.

*Corresponding author: Chunhui Zhang, E-mail: zhangchunhui@caas.cn, Tel: 86-10-62819469; Dong Han, E-mail: orange_1101@126.com, Tel: 86-10-62815950

Abstract： Perilla leaf can effectively remove off-flavours from meat cuisine, but its mechanism of action is still unclear. The effects of three characteristic aroma-active compounds (CAACs) on the structure of myofibrillar proteins (MPs) were studied. The interactions between CAACs, off-flavour compounds (OFCs) and MPs were explored. CAAC can reduce the adsorption of OFCs on MPs. Under the action of CAAC, the α-helix structure content of MPs decreased, and the content of random coil structure increased, resulting in the aggregation of MPs, which enhanced the exposure of negative charges on the surface of MPs and the zeta potential decreased from 4.52 mV to 7.5 mV. At this time, the binding interaction between OFCs and MPs weakened, resulting in the extrusion of OFCs. Fluorescence spectroscopy analysis found that the fluorescence signal of MPs was quenched after the addition of CAAC, and the connection between CAAC and MP was mainly through hydrophobic interaction. Molecular dynamics simulation showed that the average binding energy of geraniol was -7.69644 kcal/mol, which was stronger than the average binding energy of hexanal to protein (-4.67025 kcal/mol). Some binding sites on MPs partially overlapped with hexanal, and hexanal that originally bound to MPs were replaced by CAAC. In summary, CAAC molecules compete with hexanal for binding sites by changing the conformation of MPs, thereby reducing the binding rate of hexanal. This study provides new ideas for studying the off-flavour removal mechanism of spices.

Keywords: off-flavour removal, myofibrillar protein, molecular dynamics simulation, hydrophobic interaction, competitive binding site

1. Introduction

Chicken is a key ingredient in many meat cuisines (MC) worldwide, valued for being a low-fat, high-protein choice. However, there are some typical chicken off-flavours which affect consumer acceptance (Wang et al., 2018a). Perilla leaves (PL) are often used as a cooking condiment to remove meat off-flavour in MC (Fu et al., 2024; Huang et al., 2023; Kasahara & Osawa, 2008). Especially during food processing, PL can effectively remove fishy and off-flavour smells from meat or fish and improve the overall flavour. The antioxidant properties of perilla leaves can also help reduce off-flavours caused by oxidation reactions in food and prevent rancidity and greasiness caused by fatty acid oxidation (Zhao et al., 2019). It has been reported that PL can inhibit the generation of off-flavours in surimi gel through its antioxidant properties. Meanwhile, the aroma compounds in PL enhance the flavour of surimi gel, helping to mask off-flavours (Dang et al., 2024). Adding perilla juice to meat can also reduce unpleasant smells, mainly by decreasing sulphur compounds (Fu et al., 2024). In summary, as a traditional Chinese medicinal material and common food condiment, PL play an indispensable role in enhancing food flavour and removing off-flavour.

Myofibrillar proteins (MPs) are an effective carrier of volatile compounds in meat-based foods, with their adsorption and release of odour components playing a crucial role in shaping the flavour profiles of meat-based foods (Tornberg, 2005; Wang et al., 2023). Various studies have reported on the interactions between volatile compounds and MPs, mainly focusing on the forces between MPs and volatile compounds. They pointed out that interactions between terpenes and proteins are more likely to be established through non-covalent binding (Lahmar et al., 2018), whereas hydrophobic interactions are the main forces leading to protein-ketone interactions (Shen et al., 2019). Additionally, alcohols bind to proteins through forces such as hydrogen bonds, resulting in changes

in the structure of the hydration layer around the protein and the functional properties of food proteins (Xiong et al., 2024). Xue et al. (2023) used molecular dynamics simulation to elucidate the dynamic binding characteristics between odorants (hexanal, 1-octen-3-ol, nonanal) and myosin at different temperatures. It was found that the myosin head was the main binding area, and the hydrophobic interaction force was the main force. It is reported that Ince et al. (2025) increased the knowledge in the field of flavour compound and protein interaction by using molecular docking simulation to determine the binding position of proteins with aldehyde compounds. However, the mechanism by which PL removes off-flavours from MC has not yet been reported. How the characteristic aroma active compounds (CAACs) with different structures in PL induce changes in MP structure remains unclear. The potential relationship between the binding sites of these CAACs and the release of off-flavour compounds (OFCs) needs further exploration.

The sensory interactions between ingredients in a mixture are driven by chemical or physicochemical interactions, leading to subsequent changes in sensory stimulation (Berglund and Thomas, 1976). Interactions between compounds can have an inhibitory effect on the volatility of food products because intermolecular interactions are mainly controlled by van der Waals forces, supplemented by electrostatic interactions. Most authors believe that the mechanism of spice removal of off-flavours is mainly via off-flavour masking. Specifically, the aroma of spices masks off-flavours in MC, resulting in the unique aroma of MC and enhanced consumer satisfaction (Jung et al., 2024; Luo et al., 2022; Pu et al., 2022). In fact, this masking effect is related to the interaction between olfactory receptors and odour molecules. When there are competitive active sites between different odour molecules, they often show a masking effect (El Mountassir et al., 2016). Some studies have characterised the interaction between odour molecules and olfactory receptors (Jung et

al., 2024; Luo et al., 2022; Pu et al., 2022). However, the interaction between odour molecules has not been reported. In addition to the interaction between proteins and odour molecules, whether there is an interaction between odour molecules that affects off-flavour removal is worthy of further study.

Currently, several OFCs have been identified in chickens by GC-O-MS analysis, including hexanal, heptanal, nonanal, 1-octen-3-ol, benzaldehyde and 1-pentanol. Aldehydes, such as hexanal, heptanal and nonanal, are also considered potential off-flavour substances in poultry products (Fruet et al., 2018; Jia et al., 2021; Przybylski et al., 2021). D-Limonene, acetophenone and geraniol were selected from PL, which have been detected in many spices and are unique plant-derived aroma-active compounds (Hirai et al., 2022; Lin et al., 2024; Malik & Rawat, 2021; Seo & Baek, 2009; Yang et al., 2024). The HS-SPME results showed that the addition of CAACs significantly increased the percentage of OFCs, including hexanal, heptanal, nonanal, 1-octen-3-ol, benzaldehyde, and 1-pentanol ($P < 0.05$). This showed that OFCs are not simply removed by masking flavour, and the molecular mechanism needs further exploration. This study initially analysed changes in protein structure using surface hydrophobicity, total thiol content, particle size, zeta potential, scanning electron microscopy (SEM) and atomic force microscopy (AFM). Fourier transform infrared spectroscopy (FT-IR) and fluorescence spectroscopy were used to understand the interactions between these CAACs and MPs. Secondly, this study investigated the interactions between odour molecules (CAACs and OFCs) and their impact on off-flavour removal. Lastly, molecular dynamics (MD) simulations were conducted to observe whether these CAACs and OFCs bind competitively with MP sites. The off-flavour removal mechanisms of these three CAACs were elucidated from these perspectives, offering new insights into the study of off-flavour removal in spices.

2. Materials and methods

2.1 Materials and chemicals

Fresh three-yellow chicken breasts were obtained from a local supermarket (Weize Fresh Supermarket, Beijing, China). External fat was completely removed, and the muscles were cut into small pieces for protein extraction.

Hexanal (95%), nonanal (99.5%), octanal (99%), benzaldehyde (99.5%), 1-pentanol (95%), 1-octen-3-ol (95%), geraniol (99%), D-limonene (98%), acetophenone (99.6%) and 2-methyl-3-heptanone (99%) standards were purchased from Sigma-Aldrich (Sigma Aldrich, St. Louis, MO, U.S.A.). Other chemicals were purchased from Sinopharm Chemical Reagent Beijing Co. Ltd. (Beijing, China).

2.2 Extraction of MPs

MP extraction was performed according to a previously published method with slight modifications by Sun et al. (2023). Chicken breasts were minced and mixed with four volumes (w/v) of phosphoric acid extract (0.1 mol/L NaCl, 2 mmol/L $MgCl_2$, 1 mmol/L EGTA, 10 mmol/L K_2HPO_4, pH 7.0). Homogenization was repeated three times at 15,000 rpm for 30 s, followed by centrifugation for 15 min (2000 × *g*, 4℃). The supernatant was discarded and the precipitate collected. The phosphoric acid extract was added to the precipitate and the mixture centrifuged three times. Subsequently, the precipitate was washed three times with four volumes (w/v) of 0.1 mol/L NaCl. The connective tissue was removed by gauze filtration, and the pH was adjusted to 6.0 with 0.1 mol/L HCl. The resulting precipitate was the MP. The BCA protein assay kit (Thermo Fisher Scientific Inc., Waltham, USA) was used to determine the protein concentration.

2.3 Preparation of CAAC-MP mixtures

Sample preparation followed the method of Sun et al. (2023). Solutions of the key CAACs

(geraniol, D-limonene, and acetophenone) were prepared in methanol at 1 mg/mL. These were then mixed with a 2 mg/mL MP solution to achieve a final CAAC concentration of 10 mg/g protein.

2.4 Descriptive quantitative analysis (QDA)

Our institution granted ethical permission to conduct this human sensory study. The QDA used in this study was based on the methods described by Feng et al. (2018) and Chen et al. (2023) with some modifications. The evaluation was conducted under white light at a fixed temperature of 26±2℃. The sensory panel comprised 24 evaluators (12 males and 12 females), all of whom have been engaged in flavour-related research for more than 3 years from the Meat Dish Processing Technology Integration Laboratory of the Ministry of Agriculture and Rural Affairs, Beijing, China. Membership of the sensory panel was entirely voluntary. Panellist rights and privacy were protected in accordance with ethical guidelines. All samples were verified to be non-toxic and safe for human use. The panellists were fully informed of the requirements and risks of the study and gave their consent. All details about the sensory assessors were kept confidential. Judges were required to fast for at least 3 hours and be in a good physical and mental state to evaluate the aroma changes of the chicken. The evaluation was divided into three steps.

Step 1: 2 g meat from each of the MG (marinated group) and NMG (non-marinated group) was weighed and placed in a sensory olfactory bottle (Takasago, Japan), and the panellists were left to discuss and confirm the odour description labels. The odour labels included meaty, caramel, herbal, oily, stable smell and fishy.

Step 2: Food references were provided to the panellists to reach a mutual agreement on the meaning and strength of each descriptor. The food references were prepared as follows: meaty (cooked chicken, size: 1 × 1 × 0.5 cm^3, intensity 3.0), caramel (caramel popcorn, weight: 2 g, intensity 3.0), herbal (mint flavour, weight: 2 g, intensity 2.5), oily (chicken fat, weight: 2 g,

intensity 2.5), stable smell (leather, weight: 2 g, intensity 2.5), fishy (raw chicken off-flavour, weight: 2 g, intensity 2.5).

Step 3: All panellists scored the intensity of the odour description labels, and each label was evaluated in the range of 0–3 points, with 0.5 steps. The two groups of samples were sealed in triplicate in 20 mL olfactory bottles to prevent odours from escaping. Each sample was evaluated using a randomised complete block design (RCBD). Aroma assessors were blinded to the sample identities, with each assessor evaluating each sample three times. The final score was based on the average of the three individual evaluations.

2.5 Analysis of adsorption characteristics

Referring to the method by Wang et al. (2023) with some modifications, the three CAACs were dissolved in methanol to obtain a 0.5 mg/L stock solution. Subsequently, the stock solution was added to the protein solution (20 mg/mL) and the control solution (PBS buffer, containing 0.6 M NaCl, pH 6.0) to obtain a final concentration of 0.5 mg/L for each aroma compound. Then, 5 mL of the mixture was transferred to a 20 mL headspace vial, which was sealed with a polytetrafluoroethylene-faced silicone septum and then stored at 4°C for 12 h to reach equilibrium.

To extract volatile compounds, a carbon/polydimethylsiloxane (CAR/PDMS) fibre (75 μm, 2 cm; Supelco, Bellefonte, PA) was used at 25°C for 30 min. Volatile analysis was performed using a QP2010 Plus GC-MS (Shimadzu Corporation, Kyoto, Japan) equipped with a DB-Wax capillary column (30 m × 0.18 mm × 0.18 μm; Agilent Technologies, Santa Clara, CA). GC-MS parameters included helium (99.99%) as the carrier gas, a flow rate of 1 mL/min, an ionization energy of 70 eV and a scan range of 40–500 m/z. The column temperature was maintained at 40°C (3 min), increased from 40°C to 50°C (2 °C/min), then from 50°C to 80°C (4 °C/min) and then from 80°C to 230°C (10 °C/min) for 10 min. The percentage of OFCs was calculated using equation (1) as follows:

$$\text{Percentage of OFC (\%)} = \frac{S_1 - S_0}{S_0} \times 100\% \quad (1)$$

Where S_1 is the peak area of OFCs after adding CAACs, and S_0 is the peak area of OFCs.

2.6 The impact of CAACs on MP structure and its interactions with MPs

2.6.1 Surface hydrophobicity determination

Surface hydrophobicity was measured according to a previous study by Chelh, Gatellier, and Santé-Lhoutellier (2006). Briefly, the MP solution was diluted to 5.0 mg/mL with PBS buffer (0.6 mol/L NaCl, pH 6.0). Bromophenol blue (BPB, 1 mg/mL, 20 μL) was added to the sample and centrifuged (4000 × *g*, 10 min, 4°C), and the supernatant was centrifuged again under the same conditions. Finally, the absorbance of all samples was measured at 595 nm relative to the blank (PBS buffer).

2.6.2 Total sulfhydryl content determination

The total sulfhydryl content of samples was determined according to the method described by Wang et al. (2018b) with some modifications. After diluting the sample to 1 mg/mL with PBS buffer (0.6 mol/L NaCl, pH 6.0), 0.5 mL of the sample was mixed with 4.5 mL of buffer (10 mmol/L EDTA, 0.1 mol/L KH_2PO_4), and finally 2-nitrobenzoic acid (0.1%, 100 μL) was added and incubated at 40°C for 30 min. After cooling to room temperature, the absorbance at a wavelength of 412 nm was measured by using a Synergy H_1 microplate reader (BioTek, Winooski, Vermont).

2.6.3 Particle size and zeta potential measurements

The MPs solution was analysed at 25°C using a zeta potential meter (Zetasizer Nano Zs, Malvern, UK). Referring to a previous study by Wang et al. (2023), the protein concentration was adjusted to 1 mg/mL using PBS buffer (0.6 M NaCl, pH 6.0) before the particle size and zeta potential measurement. The relative refractive index and absorption index were set to 1.414 and 0.001, respectively.

2.6.4 Scanning electron microscopy (SEM)

A scanning electron microscope (SU3500, Hitachi, Japan) was used to observe the microstructure of the samples. The freeze-dried samples were covered with a layer of gold under vacuum. Each sample was acquired at an accelerating voltage of 10 kV at an appropriate magnification.

2.6.5 Atomic force microscopy (AFM)

The prepared samples were dropped onto mica sheets and analysed using NX10 (Park Systems Ltd., Korea). The samples were scanned and recorded with a resolution of 256 × 256 and a scan area of 2.5 μm × 2.5 μm.

2.6.6 Fourier transform infrared spectroscopy (FT-IR) measurements

FT-IR analysis was performed according to a previous study with some modifications by Kaur et al. (2018). Sample powder (0.5 mg) and KBr (50 mg) were mixed, compressed and scanned using a Fourier transform near-infrared spectrometer (TENSOR 27 (ATR), Germany). The test was performed in the scanning range 4000–400 cm^{-1}, at a scanning speed of 4 cm^{-1}. The infrared spectrum was Fourier deconvoluted using PeakFit 4.12 software (SeaSolve Software, USA), and the protein secondary structure (α-helix, β-fold, β-turn and random coil) content was calculated according to Kong and Shaoning (2007).

2.6.7 Fluorescence spectroscopy

Fluorescence spectra were obtained according to previously published methods with slight modifications (Wang et al., 2018c). CAAC-MP solutions were diluted to 0.5 mg/mL protein with PBS buffer (0.6 mol/L NaCl, pH 6.0) and then scanned at three different temperatures (25°C, 35°C and 45°C) using a fluorescence spectrophotometer (BioTek Synergy H1, Agilent Technologies, Inc.,

California, USA). The experimental conditions were as follows: excitation wavelength 280 nm, wavelength range 310–450 nm, scan rate 300 nm/min and slit width 5 nm.

The quenching mechanism was further evaluated using the Stern-Volmer equation (2). The binding constant (K_a) and binding sites (n) were calculated using formula (3).

$$\frac{F_0}{F}=1+K_{sv}[Q]=K_q\tau_0[Q] \quad (2)$$

$$\lg\left[\frac{F_0-F}{F}\right]=\lg K_a+n\lg[Q] \quad (3)$$

In formula (2), F_0 and F represent the fluorescence intensity of MPs with and without CAACs, respectively, while Q is the quencher concentration, $\tau 0$ (10^{-8} s^{-1}) is the lifetime of the fluorophore without quencher and K_q and K_{sv} are the bimolecular quenching rate constant and Stern-Volmer quenching constant, respectively.

The Van't Hoff equation (4) and (5) were used to calculate ΔH (enthalpy change), ΔS (entropy change) and ΔG (free energy change) during the interaction between MPs and OFCs.

$$\ln K_a=-\frac{\Delta H}{RT}+\frac{\Delta S}{R} \quad (4)$$

$$\Delta G=\Delta H-T\Delta S \quad (5)$$

where T is the absolute temperature, R is a constant (8.314 J/ mol·K) and K_a is the quenching constant at the corresponding temperature.

2.7 Analysis of odour molecule interactions

Stock solutions (50 mM) of OFCs and CAACs were prepared. OFC and CAAC stock solutions (2.5 mL) were placed in a 20 mL headspace bottle, and 2.5 mL of OFC stock solution and 2.5 mL of phosphate buffer (0.6 mol/L NaCl, 50 mmol/L Na_2HPO_4/ NaH_2PO_4, pH 7.0) were used as controls. The equilibrated samples were adsorbed at 25℃ for 30 min and desorbed at 250℃ for 5 min. The changes in OFCs in the headspace were observed by GC-MS analysis. GC-MS parameters referred to those described in Section 2.5.

2.8 MD simulation

2.8.1 Protein homology modelling

Due to the complex nature of MPs, it is challenging to achieve unity in computational modelling. Myosin accounts for a large part of MPs (55%–60% of its total composition) and has a superior adsorption capacity for odour compounds compared to other proteins in MPs. Therefore, myosin was chosen as a reasonable representative of MD, and this choice was confirmed by many previous studies (Sun et al., 2024b; Han et al., 2022; Yu et al., 2023). In the RCSB Protein Data Bank (PDB), a comprehensive sequence similarity search based on amino acid sequences indicated the absence of an exact match for the myosin protein crystal structure. However, the database includes a crystal structure with 81.54% sequence similarity (RCSB PDB ID: 8Q6T), which is suitable for use as a template in homology modelling. Consequently, this structure was employed for single template-based homology modelling of the chicken-derived myosin protein. In the protein's structure, the segment spanning amino acids 1–844 constitutes a conserved head domain (myosin heavy chain, MHC), while the region from amino acids 844–1940 features an elongated helical domain (myosin light chain, MLC) (Fig. S1). Among these, MHC contained the major amino acid sequence and thus possessed a similar ability to intact myosin, whereas the light chain primarily plays a regulatory role. A large number of studies and experiments have shown that the dynamic properties of myosin are mainly determined by its head region, and there are relatively mature modeling methods, such as the Brownian ratchet model and the Huxley-Simmons model, which are all based on the head region (Waller et al., 1995; Bagshaw, 2000; Zhang et al., 2020a). Therefore, the selection of this region can be compared and verified with existing research results to improve the reliability of the model. The sequence spanning amino acids 1–960 of the chicken-derived myosin protein was selected for analysis (Fig. S2). The myosin protein segments within the 1–960

amino acid region was subjected to modelling, resulting in the generation of Ramachandran plots. As shown in Fig. S3, 94.50% of the amino acids in the homology-modelled myosin fall within the Ramachandran-favoured regions. Additionally, 98.7% of these amino acids are located within the permissible regions, satisfying the structural criteria for modelling. This positions the model as suitable for further analysis.

2.8.2 MD simulation methodology

MD simulations were performed using Gromacs 2021.5 according to Zhao et al. (2024). The number of compounds bound to the protein was uniformly set to 40. First, 40 hexanal molecules were randomly deployed around the protein, then the protein system was subjected to MD simulation at 26°C for 180 ns, and the simulation was terminated. The structure of the myosin-hexanal molecular complex at the 180 ns time node was extracted for subsequent binding mode analysis (Fig. S4). Then, the three different CAACs (Table S1) (each flavour represented by 40 molecules) were randomly placed around the myosin-hexanal molecular complex structure, and the complex system was constructed (Fig. S5). Random competitive initial structure construction was performed in two stages. In the first stage, after adding a restraining force of −1500 kcal/mol to all heavy atoms of amino acids on the protein, the structures of the myosin-hexanal-acetophenone, myosin-hexanal-limonene and myosin-hexanal-geraniol complexes corresponding to 150 ns were extracted to examine the competitive binding state, followed by a second stage of MD simulation (Table S2). After removing the restraining force, the overall average structure of the molecule in the 180 ns state was extracted for subsequent bonding mode and differential analysis.

MD simulation was performed using the MD software Gromacs2021.5. The MD simulation time was uniformly limited to 180 ns. The entire protein system used the Amber ff99SB force field,

and the small molecule force field parameters were generated using cgenff. After the system was constructed, conventional MD simulation was performed using Gromacs2021.5. During the simulation, the system was first energy minimized, and after 500 ps equilibrium under the isothermal isovolumic ensemble (NVT) and isothermal isobaric ensemble (NPT) ensembles, a long-term production stage dynamics simulation was performed under the NPT ensemble. The simulation results were visualised using the Gromacs software embedded program and visual MD (VMD). Data such as the root mean square deviation (RMSD) and root mean square fluctuation (RMSF) were calculated using the software's integrated tools.

2.9 Statistical analysis

All experiments were repeated three times for replicability and to limit human error. Data were analysed using ANOVA followed by Duncan's test using SPSS (version 26.0, IBM Corporation) for Windows, and differences among means were significant at $P < 0.05$. Origin 2018 software was used for statistical analysis and plotting of experimental results and figures.

3. Results and discussion

3.1 Sensory evaluation

From the sensory evaluation results (Fig. 1A), it can be seen that the aroma profile of roasted chicken changed significantly ($P < 0.05$) before and after marinating with PL. Following PL addition, the fishy smell dropped from 2 points to 1 point, and the stable smell also decreased significantly ($P < 0.05$). At the same time, the unique herbal smell of PL increased the overall herbal smell of the sample. The oily smell was diminished, potentially due to the antioxidant activity of PL, which may have reduced the oxidation level in chicken (Dang et al., 2024). Interestingly, marinating with PL increased the meaty smell score, which may have been because the off-flavour of the chicken was masked, making the meaty smell more prominent.

3.2 Analysis of adsorption characteristics

The amount of OFC changed significantly after the addition of the three CAACs ($P < 0.05$) (Fig. 1B). These changes not only reflect the effect of CAAC on the structure of MP, but also reveal how this structural change changes the ability of MP to interact with OFC. Chicken contains some OFCs that cause the human body to directly perceive the presence of off-flavour in meat. After the addition of CAACs, OFC was released into the air, resulting in less off-flavour in chicken that was originally perceived. The greater the amount of OFC released, the lower the off-flavour perception. This may be because CAAC changes the structure of MP and affects the binding ability of MP and OFC (Shen et al., 2019). The interaction between protein and flavour compounds is replaced by protein-protein interaction, weakening the binding between protein and OFC (Kuehn et al., 2008). Finally, OFC is released into the air. At this time, the off-flavour in chicken is reduced, the flavour profile is changed, and ultimately affects the overall flavour characteristics of the food. On the other hand, the change in OFCs may have been due to the interaction between CAACs and OFCs. It is worth noting that CAACs vary in their ability to release OFCs, which related to their own properties and conformational changes in proteins (Liu et al., 2021). Among them, acetophenone shows the lowest release of OFCs, likely due to the location of the keto group inside the molecule. This generates a stronger steric hindrance effect, which hinders the binding of the keto group to the protein (Wang et al., 2022b), and a small amount of OFCs are squeezed out. Following geraniol addition to MPs, the relative release percentage of hexanal in OFCs was the highest, indicating that geraniol had a high capacity to release this compound. In addition, geraniol may compete with hexanal for binding sites on MPs, destroying the interaction between hexanal and MPs and ultimately leading to the release of hexanal (Sun et al., 2024a, b).

3.3 Changes in protein structure and interactions between CAACs and MPs

3.3.1 Surface hydrophobicity

Surface hydrophobicity can reflect changes in the physical and chemical state of the surface of protein molecules (Zhang et al., 2017). Following the addition of CAACs to MPs, the surface hydrophobicity of MPs was significantly reduced ($P < 0.05$) (Fig. 1C). This may have been due to the excessive swelling of MPs after the addition of CAACs, which led to MP aggregation. In addition, it may also be attributed to the binding of CAACs to the hydrophobic regions of proteins through hydrophobic interactions. Previous studies found that the addition of flavour compounds can reduce the content of hydrophobic groups on the surface of MPs, prevent hydrophobic amino acids from being exposed on the surface of MPs and cause them to be re-embedded (Guo et al., 2021; Sun et al., 2024b). Therefore, the amount of bound BPB is reduced, which is consistent with our results. Fig. 1C demonstrates that the amount of BPB bound to different compounds varies, and there are even significant differences ($P < 0.05$). This may be attributed to differences in the active groups between compounds, resulting in different binding affinities (Han et al., 2021; Liu et al., 2021).

3.3.2 Total sulfhydryl content

Jia et al. (2017) suggested that the redox state of thiol groups, functional changes of proteins and the antioxidant capacity of the systems can be elucidated by measuring the total sulfhydryl content. Adding D-limonene and geraniol to the protein did not change the total sulfhydryl content significantly ($P > 0.05$) (Fig. 1C). D-limonene is chemically stable and does not react with thiol groups as readily as strong oxidants or reducing agents at room temperature. As a result, it neither directly interacts with thiol groups nor significantly alters thiol content. At the same time, D-limonene can act as an antioxidant to prevent sulfhydryl groups from being affected by oxidative

stress, thereby maintaining the total sulfhydryl content in proteins or other sulfhydryl-containing molecules (Wang et al., 2023).

Nevertheless, geraniol can capture oxygen free radicals or other oxidants to prevent them from participating in oxidative reactions with sulfhydryl groups. Therefore, geraniol can delay the oxidation process of free sulfhydryl groups, thereby protecting sulfhydryl groups and preventing their conversion into disulfide bonds or other oxidation products (Han et al., 2022). After acetophenone addition to the protein, the total sulfhydryl content was significantly reduced ($P < 0.05$). Acetophenone could decrease the number of free sulfhydryl groups in the total sulfhydryl content directly by reacting with sulfhydryl groups through nucleophilic addition (Wang et al., 2022b).

3.3.3 Analysis of particle size and zeta potential

The zeta potential of protein can be used to characterise the surface charge and electrostatic interaction of MPs after the adsorption of CAACs (Song et al., 2013). It can be observed as shown in Fig. 1D that after D-limonene addition, the zeta potential did not change significantly ($P > 0.05$), which may be due to its structure. D-limonene does not carry a positive or negative charge, so it will not interact directly and significantly with the charged amino acid residues on the protein surface (such as negatively charged glutamic acid or positively charged lysine). After geraniol addition, the absolute zeta potential of MPs increased. The hydroxyl group of geraniols could change the charge distribution of amino acids on the surface of MPs by forming hydrogen bonds or weak interactions, thereby affecting the zeta potential of the MPs (Zhou et al., 2014). The results of adding acetophenone and geraniols were similar, but the zeta potential value of geraniol decreased more significantly ($P < 0.05$). This because the keto group of acetophenone can react with nucleophilic

groups (such as amino or sulfhydryl groups) on the surface of proteins (Shen et al., 2019), changing the charge distribution on the protein surface and thus affecting the zeta potential.

The particle size distribution can reflect the degree of aggregation of MPs after the addition of CAACs according to Jiang et al. (2024). As shown in Fig. 1D, after CAAC addition, the average particle size of MPs increased significantly ($P < 0.05$), indicating that CAAC addition causes MP aggregation. Different CAACs have different hydrophobic interactions with proteins and change the exposure of the hydrophobic area on the protein surface differently, which should be the main reason for the inconsistent particle size distribution.

3.3.4 Changes in the ultrastructure of MPs

To further observe and confirm the changes in MP microstructure after CAAC addition, the samples were analysed by SEM and AFM. As shown in Fig. 2, the untreated MP microstructure appears smooth and evenly distributed. The microstructure of the sample treated with the CAACs is significantly different ($P < 0.05$) from that of the control group. Following CAAC addition, the protein became viscous, and obvious aggregation occurred on the surface. Sun et al. (2024a) reported a similar phenomenon where obvious aggregates formed in the MP microstructure after the addition of flavour compounds.

As can be seen from Fig. 2B, the surface of the untreated MPs is relatively flat and regular, indicating that when no flavour compounds are added, the structure of the MPs is relatively stable and evenly distributed. Under the treatment of D-limonene, aggregation occurs on the surface of MPs. This may be because D-limonene causes changes in the interactions between MPs molecules, destroying the original structure of MPs. After the addition of acetophenone, the MPs showed obvious height changes and fluctuations, indicating that acetophenone caused significant looseness

and irregularity on the surface of MPs. After the addition of geraniol, the height change of MPs was the most significant and dramatic. Geraniol may have destroyed the original tight arrangement of MPs, resulting in an irregular surface structure. These aroma compounds change the microstructure of MPs by interacting with MPs. A previous study found that the interaction between flavour compounds and MPs molecules could reduce the steric hindrance between MPs molecules, ultimately leading to an increase in the tendency of MPs to self-aggregate (Xu et al., 2020). With the help of FT-IR and fluorescence spectroscopy, the interaction between the three CAACs and proteins was further analysed from the perspective of molecular configuration.

3.3.5 FT-IR analysis

FT-IR is often used to detect the interaction between molecules and proteins. The CAAC-MPs and MPs had similar FT-IR spectra (Fig. 3A), indicating that no new covalent bonds were formed following CAAC addition. This means that the interaction between the CAACs and MPs mainly occurred via non-covalent bonding interaction (Huang et al., 2022b).

The α-helix structure is primarily stabilised by intermolecular hydrogen bonds between the C=O and N-H groups (Cao et al., 2019). Upon CAAC addition, the α-helix content decreased to varying extents, whereas the random coil content increased (Fig. 3B). Notably, the α-helix content decreased more than that of acetophenone and D-limonene. These compounds interact with the amino acid residues in the polypeptide chain of MPs, disrupting their hydrogen bond network and breaking the intramolecular hydrogen bonds, thereby altering the protein structure (Zhang et al., 2020b). The reduction in α-helix length observed with geraniol addition may be attributed to its ability to form hydrogen bonds with the oxygen and nitrogen atoms on the protein backbone (Qi et al., 2018). Given the changes in secondary structure upon complexation of the flavour compounds

with the proteins, there appears to be a clear interaction between CAACs and MPs, as further detailed in the following section.

3.3.6 Fluorescence spectroscopy

Fluorescence quenching of proteins is a useful method to investigate changes in the tertiary structure of proteins after the addition of CAACs (Dou et al., 2021). As shown in Fig. 4, the fluorescence intensity decreases with increasing concentrations of CAACs, indicating significant alterations in the tertiary structure of MPs. This change could result from protein unfolding and the interaction between the flavour compounds and fluorophore-containing residues (Huang et al., 2022a).

To further explore the type of fluorescence quenching between CAACs and MPs, the Stern-Volmer equation was applied to analyse the quenching data. The K_q value obtained was much higher than the maximum dynamic quenching rate constant (2.0×10^{10} $L \cdot mol^{-1}$ s^{-1}), suggesting that the fluorescence quenching mechanism is static quenching. This static quenching occurs due to molecular binding, forming a complex, rather than dynamic quenching resulting from molecular diffusion and collision (Yu et al., 2023). Additionally, the calculated n value from formula (3) was close to 1 (Table S3), indicating that CAACs bind to a single site on MPs. Among the CAACs, D-limonene, which contains hydroxyl and carbon-carbon double bonds, is more likely to form a larger electron-deficient system and bind more readily to proteins, compared to the carbon-carbon double bond in geraniol and the ketone group in acetophenone (Jin et al., 2012). Moreover, tryptophan, tyrosine, and phenylalanine residues tend to bind to molecules with insufficient charge, as the π-electron cloud in their binding cavity forms an electron transfer complex (Liu et al., 2005). Hydrophobic interactions are the primary forces driving the formation of D-limonene-MPs,

geraniol-MPs and acetophenone-MPs complexes ($\Delta H > 0$ and $\Delta S > 0$). Furthermore, the interaction between CAACs and MPs is spontaneous ($\Delta G < 0$). Geraniol can interact with tryptophan in myofibrillar protein. When geraniol binds to the tryptophan residue, it may cause fluorescence quenching. Similarly, acetophenone may induce fluorescence quenching by binding to the amino acid side chain (Han et al., 2022; Xiong et al., 2024). Upon binding to the protein, acetophenone forms a stable complex, leading to a decrease in the protein's fluorescence emission intensity. The ketone group has a large spatial structure, which may hinder the fluorescence radiation of the protein itself (Shen et al., 2019). This physical spatial effect also leads to a decrease in fluorescence intensity. D-limonene can interact non-covalently with the hydrophobic regions or amino acid residues of proteins. This hydrophobic effect may cause a change in protein conformation, resulting in fluorescence quenching. It has been reported that the binding of flavour compounds (FCS) in spices to MP may involve hydrophobic and electrostatic interactions. Although electrostatic interactions also exist, hydrophobic interactions are the main binding force of FCS-MP complexes (Sun et al., 2024b). This is consistent with our results.

3.4 Analysis of the interaction forces between odour molecules (OFCs and CAACs)

The interaction between CAACs and MPs was analysed above, and it was found that there were interactions between CAACs and MPs. The binding ability of the CAACs was stronger than that of OFCs, CAACs eventually replaced OFCs in binding with the protein structure and CAACs were released into the headspace. In addition to the force between the MPs and CAACs, there may also be an interaction force between CAACs and OFCs. The interaction force between odour molecules causes mutual pulling and dragging (Lechner & Sax, 2017), which may remove off-flavours. To verify whether there was an additional force between odour molecules that affected the removal of off-flavours, the interaction force between odour molecules was examined further.

As shown in Fig. 5, the addition of the three CAACs to different OFCs revealed that the difference in peak area in the headspace was not significant ($P > 0.05$), suggesting that the interactions between odour molecules do not significantly ($P > 0.05$) affect the release of off-flavours. This indicates that the interaction between CAACs and OFCs did not cause the increase in headspace off-flavour compounds. The interaction between CAACs and MPs was the main factor affecting OFC release.

3.5 MD simulation

3.5.1 Changes in secondary structure

MD simulation was used to verify the results of protein denaturation following CAAC addition. The results revealed (Fig. 6) that after the protein bound to CAACs, the protein's secondary structure changed significantly. The main changes were a decrease in α-helix content and an increase in random coil content, indicating that the protein structure became increasingly disordered. Following CAAC addition, the β-sheet content also increased, indicating that MPs aggregates at this time (Xiong et al., 2024). These research results are consistent with FT-IR experimental results.

3.5.2 Competitive binding of three CAACs to hexanal

MD simulations were run to explore the off-flavour removal mechanism of CAACs. The interactions between proteins, OFCs and CAACs were further studied from a molecular perspective. Hexanal, as a representative odour compound, is frequently reported in meat products. Hexanal has a grassy smell, and when its content is high, it will mask or affect the fresh flavour of chicken (Ren et al., 2024). In the binding capacity experiment, the release amount of hexanal was the highest. Therefore, we selected hexanal as a representative compound of OFCs for MD simulations. Forty bounds to myosin, and they were evenly distributed on its surface and in the tiny cavities inside (Fig. S4, S5). Afterwards, we constructed a simulation system of myosin-hexanal and three CAACs to

explore how the interaction between CAACs molecules and proteins can achieve the removal of OFCs. As described in Section 2.8, the entire simulation process was carried out in two stages. In the first stage, the state of CAACs and OFCs competitively binding to myosin during the simulation was analysed. As time increased, CAACs molecules gradually began to contact myosin and eventually bound stably to the myosin surface (Fig. S6, S7). When participating in the competitive binding of CAACs, acetophenone was less competitive, D-limonene was more competitive and geraniol was the most competitive. In the second stage, the structural morphology of CAACs and myosin was analysed. The changes in the binding mode between the two were studied, and the binding mode was also determined (Fig. S8).

The MMBSA energy calculation module in the AMBER software was used to calculate the energy of the molecules of the three constructed single systems binding to myosin. The binding energy and number of bound molecules (NTotal) corresponding to each system are shown in Table S4. The compound with the highest off-flavour removal efficiency was geraniol, and the average energy of binding to protein among the 40 compounds was −7.69644 kcal/mol. Finally, 35 of the 40 hexanal substances were directly squeezed out by geraniol and could not bind to the protein. The average binding energy between the remaining 5 hexanal and protein was −4.67025 kcal/mol. The above results show that the binding energy between geraniol and protein is stronger, so it can easily squeeze out the hexanal molecules. Geraniol, which has the most intense competition, shows the highest off-flavour removal efficiency, which is consistent with the results of the headspace experiment. Compared with geraniol, the off-flavour removal efficiency corresponding to D-limonene is slightly lower. Of the 40 D-limonene molecules, 37 D-limonene molecules can bind to the protein surface, and the corresponding average binding energy is −5.86735 kcal/mol. However,

it is worth noting that only 25 D-limonene molecules occupy the binding sites of the original hexanal molecules, so there are still 12 hexanal molecules that are not squeezed out and can still bind to the protein well, and the corresponding average binding energy is −4.70760 kcal/mol. Therefore, the off-flavour removal efficiency of D-limonene is low. The compound with the lowest off-flavour removal efficiency is acetophenone. Acetophenone molecules have the weakest effect in squeezing out hexanal molecules. It can be seen from Table S4 that only 34 acetophenone molecules are bound to the protein, of which 25 hexanal molecules are still bound to the protein and have not been squeezed out. The average binding energy of acetophenone is −5.36392 kcal/mol, but it is still higher than that of hexanal molecules, so acetophenone has the lowest efficiency. This may be due to the air steric hindrance effect of the ketone group, which limits the binding of the ketone group to the protein. The ketone groups that cannot bind to the protein fail to compete with hexanal for the protein site, ultimately resulting in a small amount of binding (Shen et al., 2019). During the entire simulation process, the number of OFCs molecules bound to myosin decreased significantly ($P < 0.05$). In addition, studies have shown that aroma compounds reduce the ability of myosin to bind to decanal, which is consistent with our results (Sun et al., 2024a).

3.5.3 Analysis of the binding modes of three CAACs and hexanal with myosin

Fig. 7 shows the interaction between CAAC, OFC and MP molecules. The binding sites of geraniol and hexanal are consistent, and the binding sites are A2-R18-E89-D90-Y118-R148-Q149-E150-P152-A151. The positions of geraniol and hexanal overlap, so that geraniol can squeeze hexanal out of the original binding site and re-bind with the protein at the same binding site. The binding sites of D-limonene and acetophenone with hexanal molecules are T335-D336-K349-Y353-L300-I292-P298-K297-L332-Q291 and V589-I470-N474-D472-K575-A576-A578-N592-D590

respectively. Fig. 8 is a detailed diagram of the mechanism of OFC removal by CAACs. After the addition of CAACs, the conformation of the protein is changed, weakening the binding between hexanal and the protein. At the same time, CAAC molecules will compete with hexanal for protein binding sites. At this time, hexanal, which has weakened its binding force with the protein, cannot compete with CAACs with stronger binding ability. As a result, hexanal is finally squeezed out and the off-flavour is eliminated.

4. Conclusion

The study found that the interaction between CAACs and MPs is the primary factor affecting the release of OFCs. The interaction between CAACs, OFCs and MPs was revealed by combining HS-SPME, multispectral analysis and MD simulation. CAACs significantly decreased the adsorption of MPs on OFCs and also reduced the surface hydrophobicity of the MPs. CAACs changed the secondary structure of MPs, causing MPs to aggregate. The aggregated surface formed uneven and rough particles, which reduced the binding force between MPs and OFCs. OFCs mainly bind to MPs through hydrophobic interactions. This finding was confirmed by MD simulation. In addition, it was found that CAACs and hexanal have competitive binding protein sites. Among CAACs, geraniol has the best off-flavour removal effect, followed by D-limonene and finally acetophenone. In general, CAACs achieve off-flavour removal mainly through two pathways: (1) CAACs induce MP aggregation by changing the secondary structure of MPs, weakening the binding force between hexanal and MPs. (2) CAACs and hexanal have the same binding sites on MPs, which triggers competition between CAACs and hexanal. CAACs have strong binding energy than hexanal, causing hexanal to be released into the air and ultimately eliminating the off-flavour. This study provides information on the mechanism of spices removing chicken off-flavour, which is beneficial

to the regulation of chicken off-flavour and improving the edible quality and commercial acceptance of meat products. In the future, the deodorization mechanism of spices can be further revealed by exploring the interaction between olfactory receptors and aroma compounds.

CRediT authorship contribution statement

Ke Bi: Conceptualization, Methodology, Investigation, Data curation, Writing—original draft. **Yue Liu**: Conceptualization, Methodology, Investigation, Data curation, Writing–original draft. **Kangyu Wang**: Software, Formal analysis, Data curation, Methodology. **Ping Yang**: Methodology, Writing-review & editing, Supervision. **Dong Han**: Supervision; Validation; Visualization. **Chunhui Zhang:** Resources, Funding acquisition, Supervision, Project administration. **Yanlu Luan:** Data curation. **Lijuan Dong:** Data curation. **Prince Chisoro:** Writing-review & editing. **Marie-laure Fauconnier:** Supervision, Validation, Writing-review & editing.

Conflict of interest statement

All authors have no relevant relationships to disclose.

Data availability

Data will be made available on request.

Acknowledgements

This work was financially supported by Xinjiang specialty roasted marinated chicken industrial conversion technology research and development and industrialization demonstration (2023B02033) and the Prepared Food R&D Innovation and Standardization Service Platform (2023TSGC0873).

References

Bagshaw, C. R. (2000). Motors in muscle: the function of conventional myosin II.

Berglund, B., B., L., U., & Thomas. (1976). Psychological processing of odor mixtures. *Psychological Review*, 83, 432-441. https://doi.org/10.10dsa37/0033-295X.83.6.432

Cao, H., Xidong, J., Daming, F., Jianlian, H., Jianxin, Z., Bowen, Y., et al. (2019). Microwave irradiation promotes aggregation behavior of myosin through conformation changes. *Food Hydrocolloids*, 96, 11-19. https://doi.org/10.1016/j.foodhyd.2019.05.002

Chelh, I., Gatellier, P., & Santé-Lhoutellier, V. (2006). Technical note: A simplified procedure for myofibril hydrophobicity determination. *Meat Science*, 74, 681-683. https://doi.org/10.1016/j.meatsci.2006.05.019

Chen, Y. P., Li, W., Yu, Y., Wang, M., Blank, I., Zhang, Y., et al. (2023). Elucidation of the impact of steaming on the key odorants of jinhua dry-cured ham using the sensomics approach. *Journal of Agricultural and Food Chemistry*, 71, 4932-4942. https://doi.org/10.1021/acs.jafc.2c08423

Fu, C. Y., Zou, Y. M., Zhang, Y. X., Liao, M. X., Chen, D. H., & Guo, Z. B. (2024). Comparison of different deodorizing treatments on the flavor of paddy field carp, analyzed by the E-Nose, E-Tongue and Gas Chromatography–Ion Mobility Spectrometry. *Foods*, 13, Article 2623. https://doi.org/10.3390/foods13162623

Dang, M., Li, W., You, J., Xiong, S., & An, Y. (2024). Perilla juice and ginger juice reduced warmed-over flavor (WOF) in surimi gels: Due to the inhibition of the formation of the WOF compounds and the masking of the WOF. *Food Chemistry*, 454, Article 139739. https://doi.org/10.1016/j.foodchem.2024.139739

Dou, P., Feng, X., Cheng, X., Guan, Q., Wang, J., Qian, S., et al. (2021). Binding of aldehyde flavour compounds to beef myofibrillar proteins and the effect of nonenzymatic glycation with

glucose and glucosamine. *LWT-Food Science & Technology*, 144, Article 111198. https://doi.org/10.1016/j.lwt.2021.111198

El Mountassir, F., Belloir, C., Briand, L., Thomas-Danguin, T., & Le Bon, A. M. (2016). Encoding odorant mixtures by human olfactory receptors. *Flavour and Fragrance Journal*, 31, 400-407. https://doi.org/10.1002/ffj.3331

Zhou, F. B., Zhao, M. M., Su, G. W., & Sun, W. Z. (2014). Binding of aroma compounds with myofibrillar proteins modified by a hydroxyl-radical-induced oxidative system. *Journal of Agricultural & Food Chemistry,* 39, 9544-9552. https://doi.org/10.1021/jf502540p

Feng, Y., Cai, Y., Fu, X., Zheng, L., Xiao, Z., & Zhao, M. (2018). Comparison of aroma-active compounds in broiler broth and native chicken broth by aroma extract dilution analysis (AEDA), odor activity value (OAV) and omission experiment. *Food Chemistry*, 265, 274-280. https://doi.org/10.1016/j.foodchem.2018.05.043

Fruet, A., Trombetta, F., Stefanello, F., Speroni, C., Donadel, J., De Souza, A., et al. (2018). Effects of feeding legume-grass pasture and different concentrate levels on fatty acid profile, volatile compounds, and off-flavor of the *M. longissimus* thoracis. *Meat Science*, 140, 112-118. https://doi.org/10.1016/j.meatsci.2018.03.008

Guo, A., Jiang, J., True, A. D., & Xiong, Y. L. (2021). Myofibrillar Protein Cross-Linking and Gelling Behavior Modified by Structurally Relevant Phenolic Compounds. *Journal of Agricultural and Food Chemistry*, 69, 1308-1317. https://doi.org/10.1021/acs.jafc.0c04365

Han, J., Du, Y., Yan, J., Jiang, X., Wu, H. T., & Zhu, B. W. (2021). Effect of non-covalent binding of phenolic derivatives with scallop (*Patinopecten yessoensis*) gonad protein isolates on protein structure and in vitro digestion characteristics. *Food Chemistry*, 357, Article 129690.

https://doi.org/10.1016/j.foodchem.2021.129690

Han, P., An, N., Yang, L., Ren, X., Lu, S., Ji, H., et al. (2022). Molecular dynamics simulation of the interactions between sesamol and myosin combined with spectroscopy and molecular docking studies. *Food Hydrocolloids*, 131, Article 107801. https://doi.org/10.1016/j.foodhyd.2022.107801

Hirai, M., Ota, Y., & Ito, M. (2022). Diversity in principal constituents of plants with a lemony scent and the predominance of citral. *Journal of natural medicines*, 76, 254-258. https://doi.org/10.1007/s11418-021-01553-7

Huang, P., Wang, Z., Feng, X., & Kan, J. (2022a). Promotion of fishy odor release by phenolic compounds through interactions with myofibrillar protein. *Food Chemistry*, 387, Article 132852. https://doi.org/10.1016/j.foodchem.2022.132852

Huang, X., Sun, L., Liu, L., Wang, G., Luo, P., Tang, D., et al. (2022b). Study on the mechanism of mulberry polyphenols inhibiting oxidation of beef myofibrillar protein. *Food Chemistry*, 372, Article 131241. https://doi.org/10.1016/j.foodchem.2021.131241

Huang, Y. Z., Ma, X. X., Zhao, W. P., Zhu, R., Zhu, B.W., & Dong, X. P. (2023). Exploring the feasibility of Spanish mackerel flavour masking process screening using preference mapping and 2D-LF-NMR. *Lwt-Food Science and Technology*, 181, Article 114736. https://doi.org/10.1016/j.lwt.2023.114736

Ince, C., Condict, L., Stockmann, R., Ashton, J., & Kasapis, S. (2025). Molecular characterisation of interactions between 11S glycinin and hexanal–An off flavour compound. Food Hydrocolloids, 158, 110543. https://doi.org/10.1016/j.foodhyd.2024.110543

Jia, N., Wang, L., Shao, J., Liu, D., & Kong, B. (2017). Changes in the structural and gel properties of

pork myofibrillar protein induced by catechin modification. *Meat Science*, 127, 45-50. https://doi.org/10.1016/j.meatsci.2017.01.004

Jia, W., Shi, Q., Zhang, R., Shi, L., & Chu, X. (2021). Unraveling proteome changes of irradiated goat meat and its relationship to off-flavor analyzed by high-throughput proteomics analysis. *Food Chemistry*, 337, Article 127806. https://doi.org/10.1016/j.foodchem.2020.127806

Jiang, S., Yang, C., Bai, R., Li, Z., Zhang, L., Chen, Y., et al. (2024). Modifying duck myofibrillar proteins using sodium bicarbonate under cold plasma treatment: Impact on the conformation, emulsification, and rheological properties. *Food Hydrocolloids*, 150, Article 109682. https://doi.org/10.1016/j.foodhyd.2023.109682

Jin, X. L., Wei, X., Qi, F. M., Yu, S. S., Zhou, B., & Bai, S. (2012). Characterization of hydroxycinnamic acid derivatives binding to bovine serum albumin. *Organic & Biomolecular Chemistry*, 10, 3424-3431. https://doi.org/10.1039/c2ob25237f

Jung, Y., Oh, S., Kim, D., Lee, S., Lee, H. J., Shin, D. J., et al. (2024). Effect of cinnamon powder on quality attributes and off-flavor in fried chicken drumsticks made from long-term thawed Korean native chicken. *Poultry Science*, 103, Article 103583. https://doi.org/10.1016/j.psj.2024.103583

Kasahara, K., & Osawa, C. (2008). Combination effects of spices on masking of odor in boiled sardine. *Fisheries Science*, 64, 415-418. http://doi.org/10.2331/fishsci.64.415

Kaur, J., Katopo, L., Hung, A., Ashton, J., & Kasapis, S. (2018). Combined spectroscopic, molecular docking and quantum mechanics study of β-casein and p-coumaric acid interactions following thermal treatment. Food Chemistry, 252, 163-170. https://doi.org/10.1016/j.foodchem.2018.01.091

Kong, J., & Shaoning, Y. U. (2007). Fourier transform infrared spectroscopic analysis of protein secondary structures. *Acta Biochimica Et Biophysica Sinica*, 39, 549-559. https://doi.org/10.1111/j.1745-7270.2007.00320.x

Kuehn, J., Considine, T. R. S., & Singh, H. (2008). Binding of flavor compounds and whey protein isolate as affected by heat and high pressure treatments. *Journal of Agricultural and Food Chemistry*, 56, 10218-10224. https://doi.org/10.1021/jf801810b

Lahmar, A., Akcan, T., Chekir-Ghedira, L., & Estevez, M. (2018). Molecular interactions and redox effects of carvacrol and thymol on myofibrillar proteins using a non-destructive and solvent-free methodological approach. *Food Research International*, 106, 1042-1048. https://doi.org/10.1016/j.foodres.2018.01.039

Lechner, C., & Sax, A. F. (2017). Towards atomic-level mechanics: Adhesive forces between aromatic molecules and carbon nanotubes. *Applied Surface Science*, 420, 606-617. https://doi.org/10.1016/j.apsusc.2017.05.170

Lin, H., Li, Z., Sun, Y., Zhang, Y., Wang, S., Zhang, Q., et al. (2024). D-Limonene: promising and sustainable natural bioactive compound. *Applied Sciences*, 14, Article 4605. https://doi.org/10.3390/app14114605

Liu, X., Song, Q., Li, X., Chen, Y., Liu, C., Zhu, X., et al. (2021). Effects of different dietary polyphenols on conformational changes and functional properties of protein-polyphenol covalent complexes. *Food Chemistry*, 361, Article 130071. https://doi.org/10.1016/j.foodchem.2021.130071

Liu, Y., Xie, M. X., Jiang, M., & Wang, Y. D. (2005). Spectroscopic investigation of the interaction between human serum albumin and three organic acids. *Spectrochim Acta A Mol Biomol Spectrosc*, 61, 2245-2251. https://doi.org/10.1016/j.saa.2004.09.004

Luo, J., Yu, Q., Han, G., Zhang, X., Shi, H., & Cao, H. (2022). Identification of off-flavor compounds and deodorizing of cattle by-products. *Journal of Food Biochemistry*, 46, Article e14443. https://doi.org/10.1111/jfbc.14443

Malik, T., & Rawat, S. (2021). Biotechnological interventions for production of flavour and fragrance compounds. *Sustainable Bioeconomy: Pathways to Sustainable Development Goals*, 7, 131-170. https://doi.org/10.1007/978-981-15-7321-7_7

Przybylski, W., Jaworska, D., Kajak-Siemaszko, K., Sałek, P., & Pakuła, K. (2021). Effect of heat treatment by the sous-vide method on the quality of poultry meat. *Foods*, 10, Article 1610. https://doi.org/10.3390/foods10071610

Pu, D., Shan, Y., Zhang, L., Sun, B., & Zhang, Y. (2022). Identification and inhibition of the key off-odorants in duck broth by means of the sensomics approach and binary odor mixture. *Journal of Agricultural and Food Chemistry*, 70, 13367-13378. https://doi.org/10.1021/acs.jafc.2c02687

Qi, J., Zhang, W. W., Feng, X. C., Yu, J. H., Han, M. Y., Deng, S. L., et al. (2018). Thermal degradation of gelatin enhances its ability to bind aroma compounds: Investigation of underlying mechanisms. *Food Hydrocolloids*, 83, 497-510. https://doi.org/10.1016/j.foodhyd.2018.03.021

Ren, Y., Wang, Y., Zhang, Y., Yang, Z., Ma, Z., Chen, J., et al. (2024). Formation and regulation strategies for volatile off-flavor compounds in livestock meat, poultry meat, and their products: A comprehensive review. *Trends in Food Science & Technology*, 152, Article 104689. https://doi.org/10.1016/j.tifs.2024.104689

Seo, W. H., & Baek, H. H. (2009). Characteristic Aroma-Active Compounds of Korean Perilla (Perilla frutescens Britton) Leaf. *Journal of Agricultural and Food Chemistry*, 57, 11537-11542.

https://doi.org/10.1021/jf902669d

Shen, H., Huang, M., Zhao, M., & Sun, W. (2019). Interactions of selected ketone flavours with porcine myofibrillar proteins: The role of molecular structure of flavour compounds. *Food Chemistry*, 298, Article 125060. https://doi.org/10.1016/j.foodchem.2019.125060

Shen, H., Zhao, M., & Sun, W., (2019). Effect of pH on the interaction of porcine myofibrillar proteins with pyrazine compounds. *Food Chemistry*, 287, 93-99. https://doi.org/10.1016/j.foodchem.2019.02.060

Song, X., Zhou, C., Fu, F., Chen, Z., & Wu, Q. (2013). Effect of high-pressure homogenization on particle size and film properties of soy protein isolate. *Industrial Crops and Products*, 43, 538-544. https://doi.org/10.1016/j.indcrop.2012.08.005

Sun, X., Li, W., Wang, Z., Yu, Y., Zhang, D., & Saleh, A. S. M. (2024a). Insights into the interactions between etheric compounds and myofibrillar proteins using multi-spectroscopy, molecular docking, and molecular dynamics simulation. *Food Research International*, 175, Article 113787. https://doi.org/10.1016/j.foodres.2023.113787

Sun, X., Yu, Y., Saleh, A. S. M., Akhtar, K. H., Li, W., Zhang, D., et al. (2024b). Conformational changes induced by selected flavor compounds from spices regulate the binding ability of myofibrillar proteins to aldehyde compounds. *Food Chemistry*, 451, Article 139455. https://doi.org/10.1016/j.foodchem.2024.139455

Sun, X., Yu, Y., Saleh, A. S. M., Yang, X., Ma, J., Li, W., et al. (2023). Understanding interactions among flavor compounds from spices and myofibrillar proteins by multi-spectroscopy and molecular docking simulation. *International Journal of Biological Macromolecules*, 229, 188-198. https://doi.org/10.1016/j.ijbiomac.2022.12.312

Tornberg, E. (2005). Effects of heat on meat proteins-Implications on structure and quality of meat products. *Meat science*, 70, 493-508. https://doi.org/10.1016/j.meatsci.2004.11.021

Waller, G. S., Ouyang, G., Swafford, J., Vibert, P., & Lowey, S. (1995). A Minimal Motor Domain from Chicken Skeletal Muscle Myosin. *Journal of Biological Chemistry*, 270, 15348-15352.

Wang, S., Zhang, Y., Chen, L., Xu, X., Zhou, G., Li, Z., & Feng, X. (2018b). Dose-dependent effects of rosmarinic acid on formation of oxidatively stressed myofibrillar protein emulsion gel at different NaCl concentrations. *Food Chemistry*, 243, 50-57. https://doi.org/10.1016/j.foodchem.2017.09.114

Wang, H., Zhang, H., Liu, Q., Xia, X., Chen, Q., & Kong, B. (2022b). Exploration of interaction between porcine myofibrillar proteins and selected ketones by GC-MS, multiple spectroscopy, and molecular docking approaches. *Food Research International*, 160, Article 111624. https://doi.org/10.1016/j.foodres.2022.111624

Wang, J., Zhao, M., Qiu, C., & Sun, W. (2018c). Effect of malondialdehyde modification on the binding of aroma compounds to soy protein isolates. *Food Research International*, 105, 150-158. https://doi.org/10.1016/j.foodres.2017.11.001

Wang, L. H., Qiao, K. N., Ding, Q., Zhang, Y. Y., Sun, B. G., Chen, H. T. (2018a). Effects of two cooking methods on the taste components of Sanhuang chicken and Black-bone silky fowl meat. *Journal of Food Processing and Preservation*, 4, e13772.

Wang, T., Han, D., Zhao, L., Huang, F., Yang, P., & Zhang, C. (2023). Binding of selected aroma compounds to myofibrillar protein, sarcoplasmic protein, and collagen during thermal treatment: role of conformational changes and degradation of proteins. *Journal of Agricultural and Food Chemistry*, 71, 17860-17873. https://doi.org/10.1021/acs.jafc.3c02618

Xiong, Z., Liu, J., Tian, Y., Wang, Z., Wang, X., Shi, T., et al. (2024). Structural and aggregation changes of silver carp myosin induced with alcohols: Effects of ethanol, 1,2-propanediol, and glycerol. *Food Chemistry*, 452, Article 139542. https://doi.org/https://doi.org/10.1016/j.foodchem.2024.139542

Yang, S. M., Chu, H. Y., Wang, Y. X., Guo, B. L., An, T. Y., & Shen, Q. (2024). Analysis of monoterpene biosynthesis and functional TPSs of Perilla frutescens based on transcriptome and metabolome. *Medicinal Plant Biology*, 3, Article e017. https://doi.org/10.48130/mpb-0024-0017

Yu, Y., Saleh., A. S. M., Sun X.X., Wang, Z.Y., Li, Y., Zhang, D. Q., et al. (2023). Exploring the interaction between myofibrillar proteins and pyrazine compounds: Based on molecular docking, molecular dynamics simulation, and multi-spectroscopy techniques. *International Journal of Biological Macromolecules*, 253, Article 126844. https://doi.org/10.1016/j.ijbiomac.2023.126844

Xu, Y. J., Zhao, Y., Wei, Z., Zhang, H., Dong, M., Huang, M., et al. (2020). Modification of myofibrillar protein via glycation: Physicochemical characterization, rheological behavior and solubility property. *Food Hydrocolloids*, 105, Article 105852. https://doi.org/10.1016/j.foodhyd.2020.105852

Xue, C., You, J., Xiong, S., Yin, T., Du, W., & Huang, Q. (2023). Myosin head as the main off-odors binding region: Key binding residues and conformational changes in the binding process. *Food Chemistry*, 403, 134437. http://doi.org/10.1016/j.foodchem.2022.134437

Zhang, B., Qi, X. E., Mao, J. L., & Ying, X. G. (2020a). Trehalose and alginate oligosaccharides affect the stability of myosin in whiteleg shrimp (Litopenaeus vannamei): The water-replacement mechanism confirmed by molecular dynamic simulation. Lwt, 127, 109393.

http://doi.org/10.1016/j.lwt.2020.109393

Zhang, L., Wang, P., Yang, Z., Du, F., Li, Z., Wu, C., et al. (2020b). Molecular dynamics simulation exploration of the interaction between curcumin and myosin combined with the results of spectroscopy techniques. *Food Hydrocolloids*, 101, Article 105455. https://doi.org/10.1016/j.foodhyd.2019.105455

Zhang, Q., Shi, J., Wang, Y., Zhu, T., Huang, M., Ye, H., … Li, H. (2022). Research on interaction regularities and mechanisms between lactic acid and aroma compounds of Baijiu. *Food Chemistry,* 397, Article 133765. https://doi.org/10.1016/j. foodchem.2022.133765

Zhang, Z., Yang, Y., Zhou, P., Zhang, X., & Wang, J. (2017). Effects of high pressure modification on conformation and gelation properties of myofibrillar protein. *Food Chemistry*, 217, 678-686. https://doi.org/10.1016/j.foodchem.2016.09.040

Zhao, Y., Kong, H., Zhang, X., Hu, X., & Wang, M. (2019). The effect of Perilla (Perilla frutescens) leaf extracts on the quality of surimi fish balls. *Food Science & Nutrition*, 7, 2083-2090. https://doi.org/10.1002/fsn3.1049

Zhao, Y., Wang, J., Zhang, Y., He, R., Du, Y., & Zhong, G. (2024). Hydration properties and mesoscopic structures of different depolymerized konjac glucomannan: Experiments and molecular dynamics simulations. *Food Hydrocolloids*, 151, Article 109853. https://doi.org/10.1016/j.foodhyd.2024.109853

Fig. 1. A. Sensory evaluation scores of roasted chickens before and after marinating with perilla leaves. B. Effect of adding different off-flavour removal compounds on the binding of CAACs to MPs. C.BPB binding and total sulfhydryl content of MPs treated with CAACs. D. Zeta potential and particle size of MPs treated with CAACs

Data represented as means ± SD of three independent experiments. Error bar represented standard deviations. Different lowercase letters indicate significant differences in odour compounds among the different treatments ($P < 0.05$); different uppercase letters indicate significant differences in odour compounds among the different treatments ($P < 0.05$).

MG, marinated group. UMG, unmarinated group.

Myofibrillar proteins, MPs. Characteristic aroma-active compounds, CAACs.

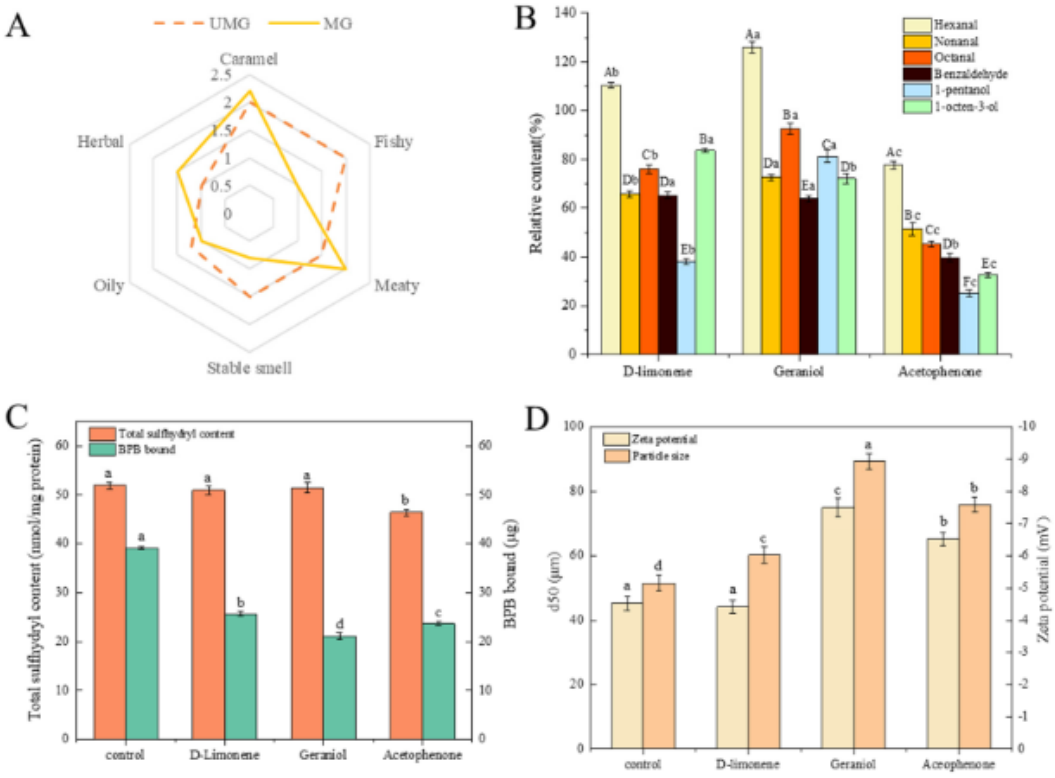

Fig. 2. Changes in MPs microstructure under different treatment conditions.

A. Scanning electron microscopy image of MPs treated with CAACs. B. Atomic force microscope image of MPs treated with CAACs.

Myofibrillar proteins, MPs. Characteristic aroma-active compounds, CAACs.

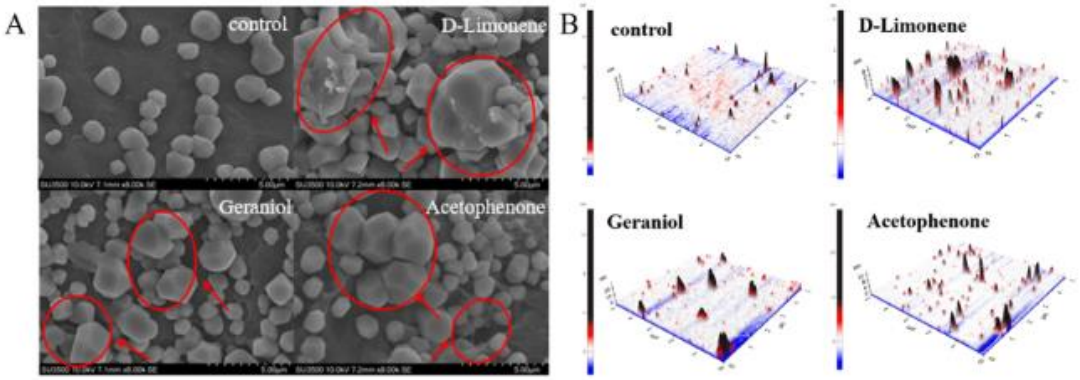

Fig. 3. FT-IR spectra (A), secondary structure (B) of MPs treated with CAACs. Data represented as means ± SD of three independent experiments. Error bar represented standard deviations (SD). Significant differences among the treatments are marked with different letters ($P < 0.05$).

Myofibrillar proteins, MPs. Characteristic aroma-active compounds, CAACs.

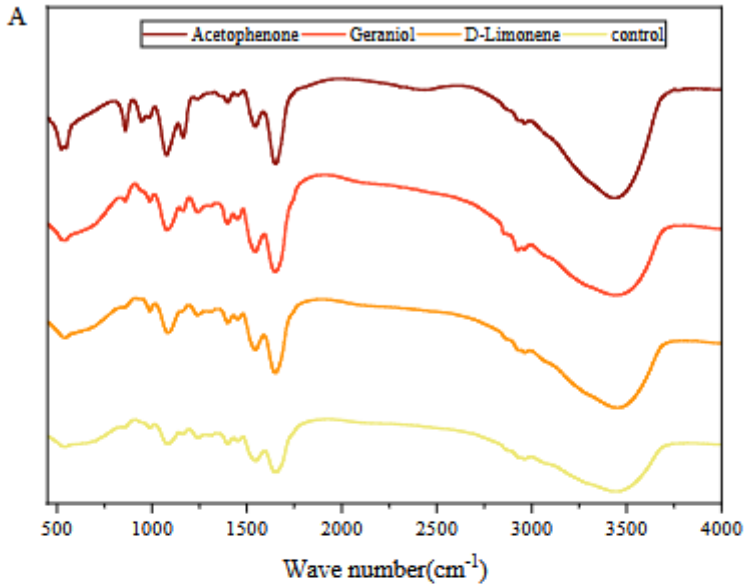
A
Acetophenone
Geraniol
D-Limonene
control
500
1000
1500
2000
2500
3000
3500
4000
Wave number(cm-1)

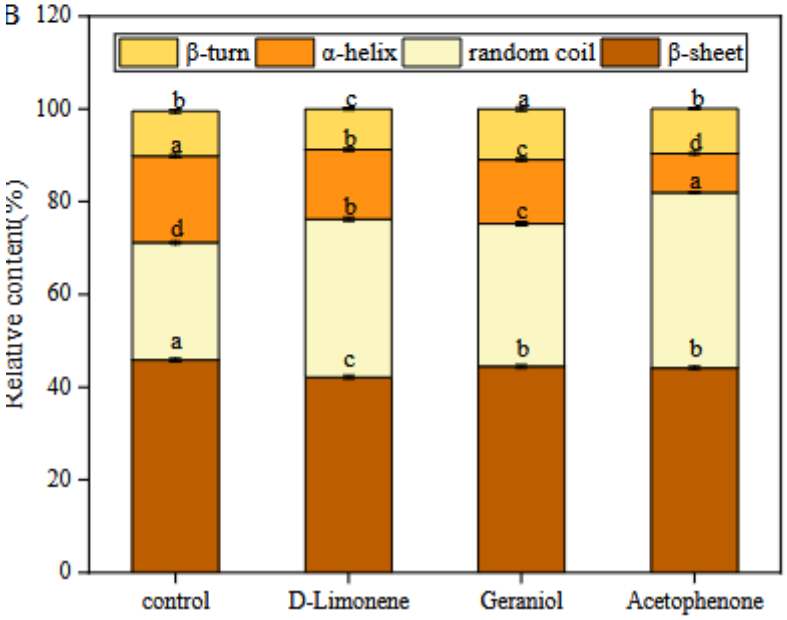
B
β-turn
α-helix
random coil
β-sheet
Relative content(%)
0
20
40
60
80
100
120
control
D-Limonene
Geraniol
Acetophenone

Fig. 4. Fluorescence quenching spectra were obtained in the presence of various concentrations of D-Limonene (A), Geraniol(B), Acetophenone(C). Stern-Volmer plots of D-Limonene (D), Geraniol(E), Acetophenone(F) at 298 K, 308 Kand 318 K.

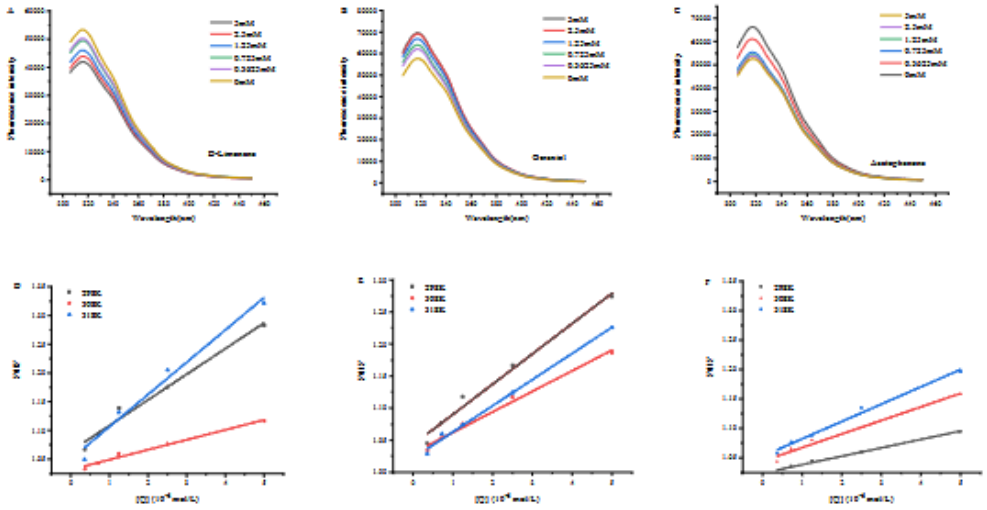

Fig. 5. Interactions between different small molecules.

Data represented as means ± SD of three independent experiments. Error bar represent standard deviations (SD). Significant differences among the treatments are marked with different letters ($P < 0.05$). Characteristic aroma-active compounds, CAACs.

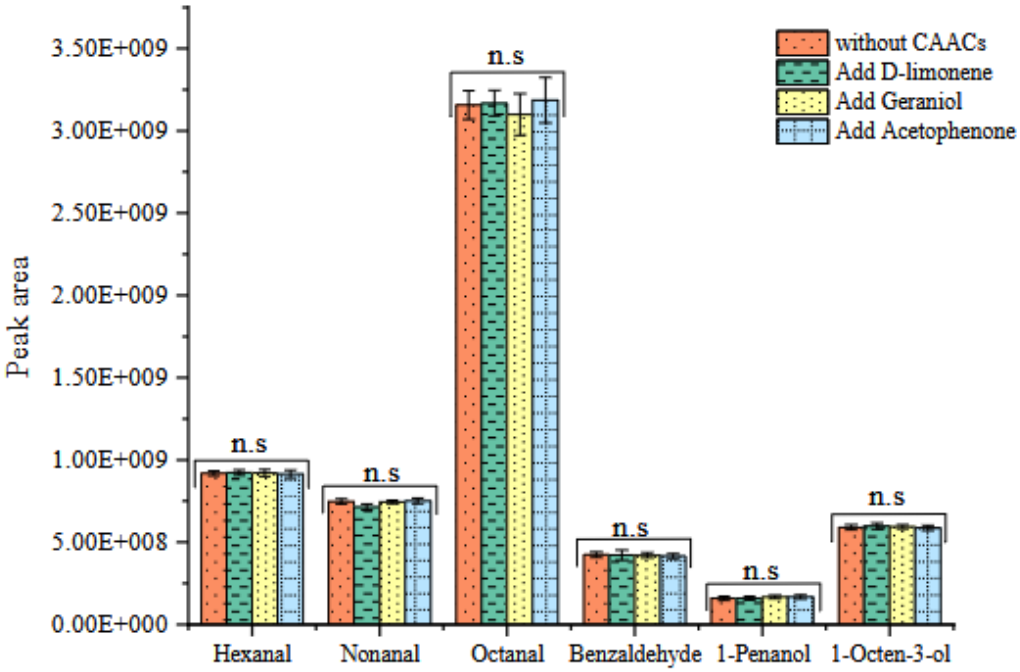

Fig. 6. Changes in protein secondary structure. A. Empty protein without small molecules. B. Geraniol-Hexanal-Myosin. C. D-limonene-Hexanal-Myosin. D. Acetophenone-Hexanal-Myosin.

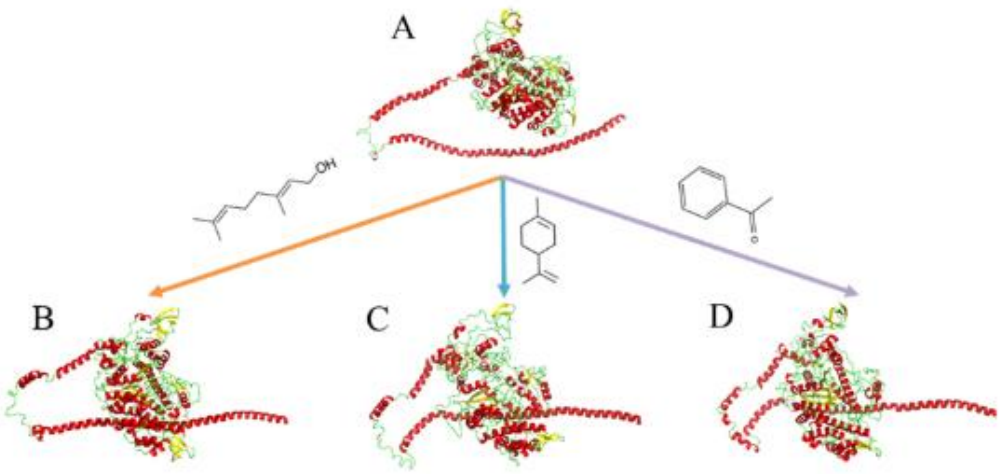

Fig. 7. Molecular interaction model of CAACs-OFCs-Myosin.

A,D,G. Geraniol-Hexanal-Myosin, B,E,H. D-limonene-Hexanal-Myosin, C,F,I. Acetophenone-Hexanal-Myosin.

Characteristic aroma-active compounds, CAACs. Off-flavour compounds, OFCs.

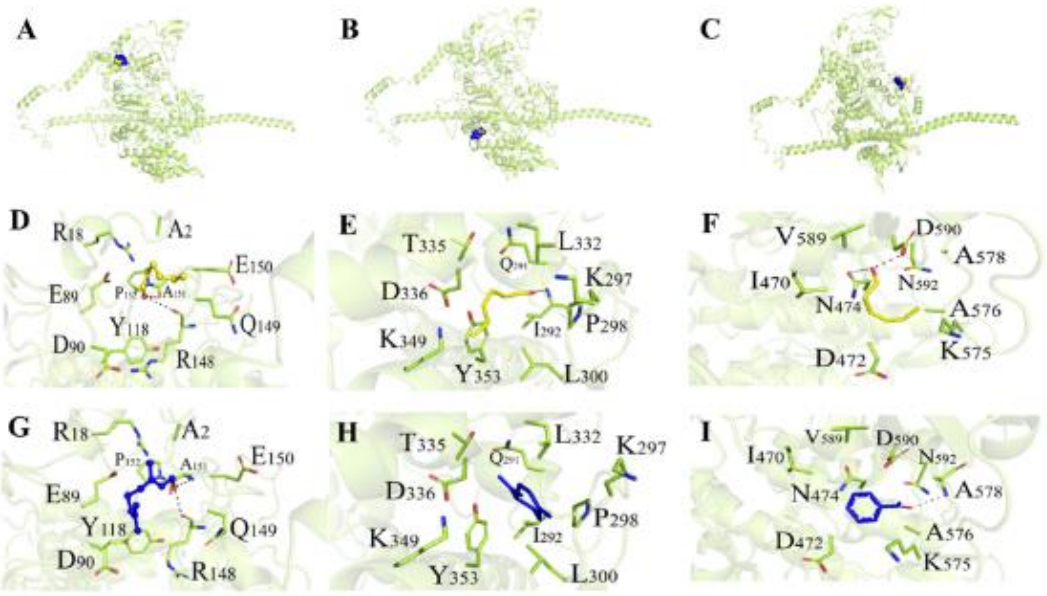

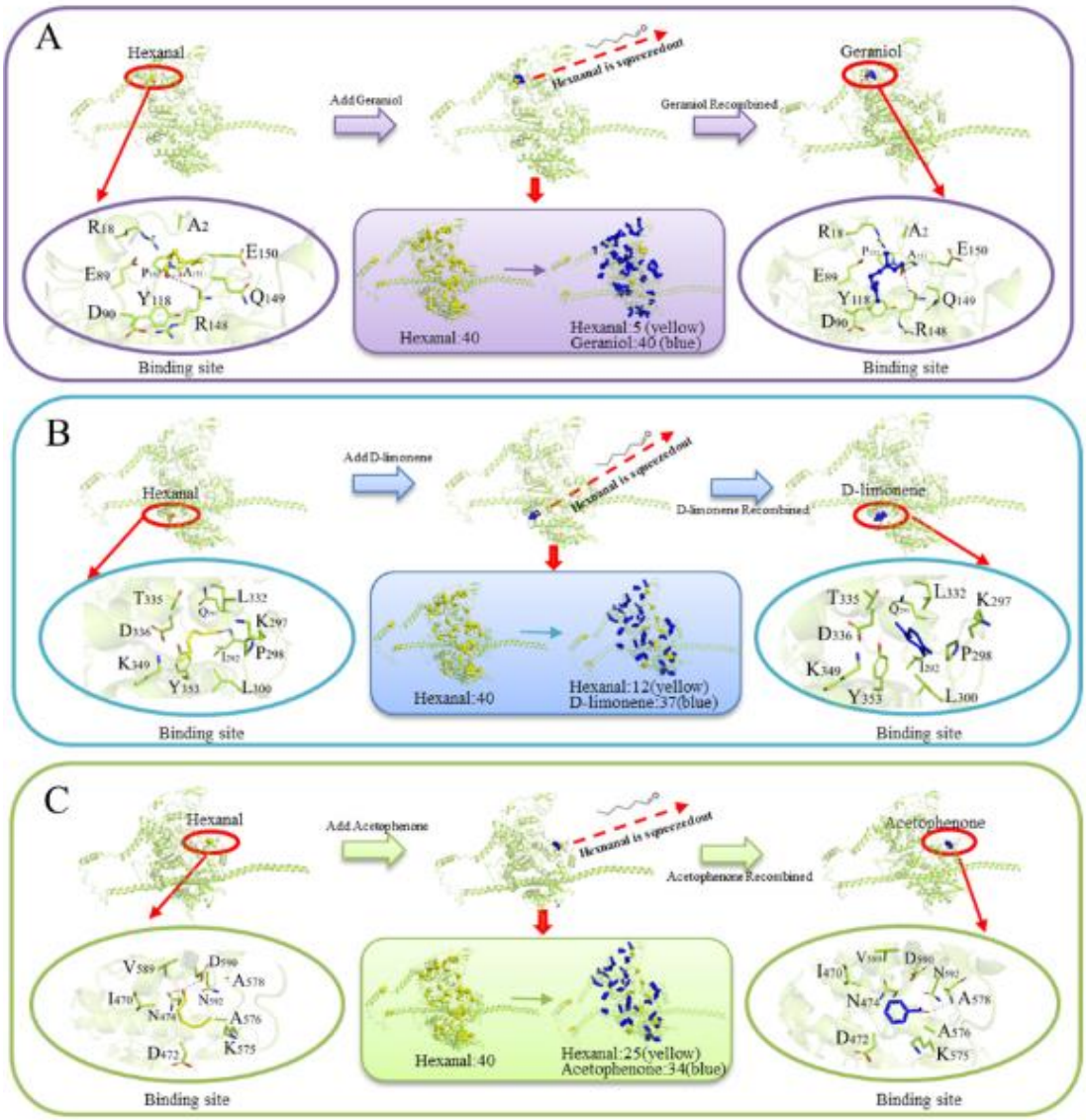

Fig. 8. Diagram of the mechanism of CAACs removing OFCs.

A. Geraniol-Hexanal-Myosin B. D-limonene-Hexanal-Myosin. C. Acetophenone-Hexanal-Myosin.

Characteristic aroma-active compounds, CAACs. Off-flavour compounds, OFCs.

Conflict of Interest

The authors have declared no conflict of interest

Corresponding author: Chunhui Zhang

Graphical abstract

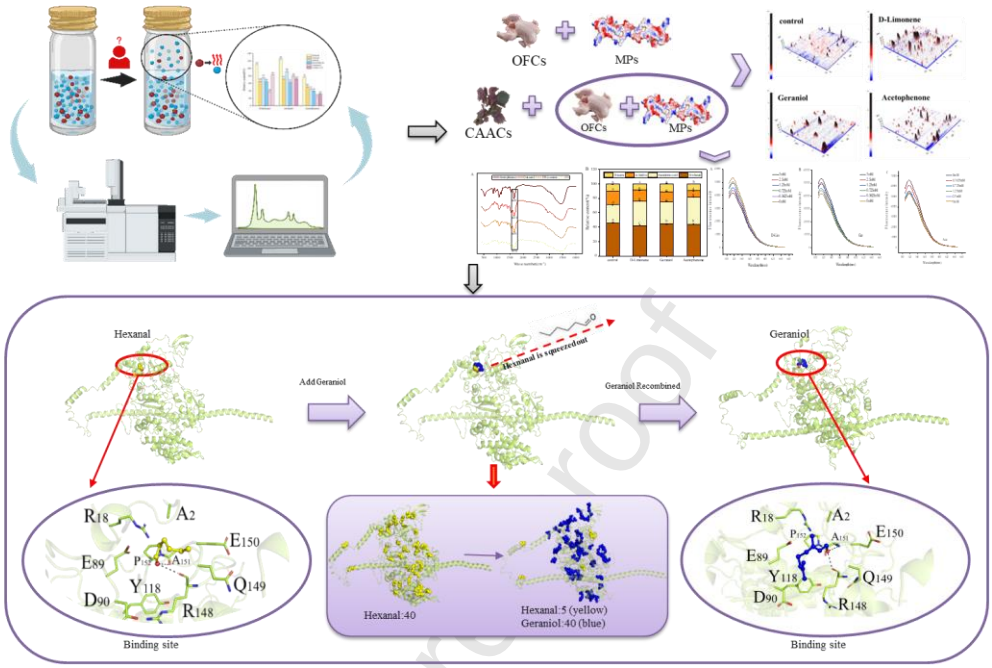

Highlights

- Deodorization mechanism of characteristic aroma-active compounds (CAACs) in perilla leaves.
- Study on the deodorization mechanism by spectroscopy and molecular dynamics.
- CAACs can trigger the release of off-flavor compounds (OFCs).
- The interaction between odor molecules does not affect the deodorization effect.
- OFCs are squeezed out after failing to compete with CAACs for protein binding sites.